Atmos. Chem. Phys. Discuss., 14, 7777–7822, 2014
www.atmos-chem-phys-discuss.net/14/7777/2014/
doi:10.5194/acpd-14-7777-2014


Atmospheric Chemistry and Physics
Discussions
Open Access



# Aerosol and dynamic effects on the formation and evolution of pyro-clouds

**D. Chang[1], Y. Cheng[1], P. Reutter[2], J. Trentmann[3], S. Burrows[4], S. Nordmann[1], M. O. Andreae[5], U. Pöschl[1], and H. Su[1]**

[1]Multiphase Chemistry Department, Max Planck Institute for Chemistry, Mainz, Germany
[2]Institute for Atmospheric Physics (IPA), Johannes Gutenberg University Mainz, Mainz, Germany
[3]German Weather Service (DWD), Offenbach, Germany
[4]Pacific Northwest National Laboratory, Richland, WA, USA
[5]Biogeochemistry Department, Max Planck Institute for Chemistry, Mainz, Germany

Received: 29 January 2014 – Accepted: 9 March 2014 – Published: 21 March 2014

Correspondence to: H. Su (h.su@mpic.de)

Published by Copernicus Publications on behalf of the European Geosciences Union.

## Abstract

A recent parcel model study (Reutter et al., 2009) showed three deterministic regimes of initial cloud droplet formation, characterized by different ratios of aerosol concentrations ($N_{CN}$) to updraft velocities. This analysis, however, did not reveal how these regimes evolve during the subsequent cloud development. To address this issue, we employed the Active Tracer High Resolution Atmospheric Model (ATHAM) with full microphysics and extended the model simulation from the cloud base to the entire column of a single pyro-convective mixed-phase cloud. A series of 2-D simulations (over 1000) were performed over a wide range of $N_{CN}$ and dynamic conditions. The integrated concentration of hydrometeors over the full spatial and temporal scales was used to evaluate the aerosol and dynamic effects. The results show that: (1) the three regimes for cloud condensation nuclei (CCN) activation in the parcel model (namely aerosol-limited, updraft-limited, and transitional regimes) still exist within our simulations, but net production of raindrops and frozen particles occurs mostly within the updraft-limited regime. (2) Generally, elevated aerosols enhance the formation of cloud droplets and frozen particles. The response of raindrops and precipitation to aerosols is more complex and can be either positive or negative as a function of aerosol concentrations. The most negative effect was found for values of $N_{CN}$ of $\sim 1000$ to $3000\,cm^{-3}$. (3) The involvement of nonlinear (dynamic and microphysical) processes leads to a more complicated and unstable response of clouds to aerosol perturbation compared with the parcel model results. Therefore, conclusions drawn from limited case studies might require caveats regarding their representativeness, and high-resolution sensitivity studies over a wide range of aerosol concentrations and updraft velocities are strongly recommended.

# 1 Introduction

Clouds have a considerable effect on the radiation, climate, and water cycle of the Earth (IPCC, 2007). Aerosol-cloud interactions are one of the most uncertain factors influencing the formation, persistence, and ultimate dissipation of clouds (Stevens and Feingold, 2009). The interplay between atmospheric aerosols, cloud water, and precipitation has been studied intensively through cloud-resolving model simulations, analysis of satellite data, and long-term observational data. However, aerosol effects are still associated with significant uncertainty in light of the seemingly contradictory results from different studies. For instance, several studies have indicated that increasing aerosol concentrations could reduce cloud fraction and inhibit cloud formation (Albrecht, 1989; Ackerman et al., 2000; Kaufman et al., 2002; Koren et al., 2004), whereas positive effects of aerosols on the cloud fraction were suggested in other studies (Norris, 2001; Kaufman and Koren, 2006; Grandey et al., 2013). Some rainfall observations have also shown such non-monotonic effects (e.g., Qian et al., 2009). Increasing aerosol concentrations may either significantly suppress the frequency and amount of precipitation (Ackerman et al., 2003, 2004; Andreae et al., 2004; Altaratz et al., 2008; Rosenfeld et al., 2008; Qian et al., 2009), or enhance the accumulated precipitation (Williams et al., 2002; Lin et al., 2006; Bell et al., 2008). Changing aerosol concentrations have also been found to exert non-monotonic influences on a wide range of cloud properties, such as homogeneous freezing (Kay and Wood, 2008), frozen water particles (Saleeby et al., 2009; Seifert et al., 2012), and convection strength (Fan et al., 2009). These contrasting results indicate that the aerosol effect is a function of many factors, including relative humidity, surface temperature, and wind shear, together with aerosol properties such as chemical composition and size distribution (Levin and Cotton, 2007; Tao et al., 2007; Khain et al., 2008; Rosenfeld et al., 2008; Qian et al., 2009). The assessment of aerosol effects also depends on the observational or analysis scales, because different scales of study result in biases in the quantification of the results (McComiskey and Feingold, 2012). Stevens and Feingold (2009) also suggested that regime-centered





ACPD
14, 7777–7822, 2014

studies are of importance, and that further work is needed to characterize the dependence of aerosol-cloud-precipitation interactions on the state of the cloud system and to improve the representation of cloud regimes in models.

While aerosol-cloud interactions appear puzzling at regional and global scales, the interplay at the microphysical scale, i.e., cloud condensation nuclei (CCN) activation, has been well characterized. CCN activation can be well predicted by the Köhler theory (Kohler, 1936) and by a series of extended equations (Shulman et al., 1996; Kulmala et al., 1997; Laaksonen et al., 1998). Simplified treatments that reduce the effects of aerosol chemistry on CCN activation to a single parameter have also proven effective; for example, the $\kappa$-Köhler equation has been demonstrated to be a practical method in the description of CCN activation and the prediction of CCN number concentrations (Petters and Kreidenweis, 2007; Su et al., 2010; Gunthe et al., 2011). When we upscale the activation of a single aerosol particle to aerosol populations at the cloud base, the impact of aerosols on the number of activated CCN still appears simple and can be well described (Conant et al., 2004; Fountoukis et al., 2007; Reutter et al., 2009; Tessendorf et al., 2013). In-situ aircraft measurements of clouds over marine and continental areas have demonstrated the significant relationship between anthropogenic aerosol concentration and cloud drop number concentration (Conant et al., 2004; Fountoukis et al., 2007). Reutter et al. (2009) implemented observationally-constrained CCN activation microphysics into parcel models, and they found three generic regimes of CCN activation at the cloud base (Fig. 1). The question remains, if CCN activation (microphysical scale) and initial warm cloud formation (air parcel scale) can be described accurately, why is it so difficult to describe the interaction at regional and global scales (Stevens and Feingold, 2009)? In particular, to what extent does complexity arise from the inclusion of other hydrometeor types, such as frozen particles and relevant microphysical processes during subsequent cloud evolution? At which scale do the aerosol-cloud interactions become complex? These questions are the first motivation for this study. Another motivation is to provide a complementary explanation to the ongoing debate over whether clouds are insensitive to aerosol particles, rendering aerosols even "ir-





ACPD
14, 7777–7822, 2014

relevant" to the climate problem (Karydis et al., 2012; Carslaw et al., 2013; Stevens, 2013). Furthermore, we may be able to distinguish under which conditions cloud formation is aerosol-limited or updraft-limited as discussed in Reutter et al. (2009). If this could be accomplished, it would have the advantage that in future work one could for many purposes neglect aerosol effects on clouds in areas that are usually updraft limited.

Biomass burning generates significant amounts of smoke aerosols, and the fires loft soil particles that contain minerals (Pruppacher and Klett, 1997), both of which could serve as effective CCN and ice nuclei (IN) (Hobbs and Locatelli, 1969; Hobbs and Radke, 1969; Kaufman and Fraser, 1997; Sassen and Khvorostyanov, 2008), thereby affecting the formation of clouds and precipitation. Mostly because of human activities, the risk of wild fires has increased significantly, especially during the last two decades, and they are identified as an important source of atmospheric aerosols (Reid et al., 2005; Luderer et al., 2006; Trentmann et al., 2006; Rosenfeld et al., 2007; Fromm et al., 2008). As an extreme consequence of biomass burning, pyro-clouds feed directly from the smoke and heat released from fires (Andreae et al., 2004; Luderer, 2007) and provide a good example with which to study aerosol-cloud interactions (Reutter et al., 2009). Luderer (2007) systematically simulated the evolution of pyro-cumulonimbus clouds (pyroCb) caused by a forest fire and performed sensitivity studies on the response of convective dynamics to the release of sensible heat by the fire, meteorological conditions, and ambient aerosols. Their results were consistent with observations, and illustrated that fire heating and large-scale meteorological conditions played an important role in the formation and transport of pyroCb. Li et al. (2008) investigated the response of clouds and precipitation to different aerosol concentrations in a convective cloud event with a two-moment bulk microphysical scheme, and found that the aerosol effects on the cloud system varied under different meteorological and aerosol conditions, due to the complicated interactions between cloud microphysics and dynamics. In these previous studies, only a few sensitivity cases were studied. Within our work, we have developed a more complete understanding of these interactions by conducting





ACPD
14, 7777–7822, 2014

over 1000 simulations, allowing us to study whether the responses of the hydrometeors to aerosol and dynamic forcing have continuity, and the reasons behind this behavior.

In this study, we used the Active Tracer High Resolution Atmospheric Model (ATHAM) to study the impact of aerosols on a single pyro-convective cloud under various dynamic conditions. The single convective clouds represent the up-scaled cases closest to the parcel model simulation. A process scale with resolution of ca. 1 km has been suggested as the appropriate scale at which to characterize processes related to aerosol-cloud interactions (McComiskey and Feingold, 2012). In addition to cloud droplets, precipitable hydrometeors (raindrops, ice, snow, graupel, and hail) were also included in the study and their responses to aerosols examined. For a better understanding of the mechanisms, we employed the process analysis (PA) method, which has been widely utilized to investigate the formation and evolution of gaseous pollutants and particulate matter (Tonse et al., 2008; Yu et al., 2009; Liu et al., 2010). The PA calculates the time-integrated rate of change in the mass or number concentration of each hydrometeor type caused by a particular process, thereby enabling the determination of the relative importance of the major microphysical processes under different dynamic forcing and aerosol conditions.

## 2 Design of numerical experiments

### 2.1 ATHAM: model and configuration

ATHAM is a non-hydrostatic model that we used to study both cloud formation and evolution in response to changes in updrafts and aerosol particle concentration. ATHAM was designed initially to investigate high-energy plumes in the atmosphere and applied to simulate volcanic eruptions and fire plumes (Herzog, 1998; Oberhuber et al., 1998). The model comprises eight modules: dynamics, turbulence, cloud microphysics, ash aggregation, gas scavenging, radiation, chemistry, and soil (Herzog et al., 1998, 2003; Oberhuber et al., 1998; Graf et al., 1999). Cloud microphysical interactions are





ACPD
14, 7777–7822, 2014

represented by an extended version of the two-moment scheme developed by Seifert and Beheng (2006), which includes the hail modifications by Blahak (2008), and is able to predict the numbers and mass mixing ratios of six classes of hydrometeors (cloud water, ice crystals, raindrops, snow, graupel, and hail; detailed in Table S1) and water vapor. It has been validated successfully against a comprehensive spectral bin microphysics cloud model (Seifert et al., 2006). The cloud nucleation (CCN activation) module is based on the lookup table derived from parcel model simulations for pyro-convective clouds (Reutter et al., 2009).

As our main purpose was to demonstrate a general pattern of sensitivity of clouds and precipitation to a wide range of aerosol concentrations ($N_{CN}$) and updrafts (represented by the intensity of fire forcing, which triggers updraft velocities), we performed two-dimensional simulations rather than the more expensive three-dimensional runs. The fire forcing and meteorological conditions were set up to simulate the Chisholm forest fire (Luderer, 2007; Rosenfeld et al., 2007), which is a well-documented case of pyro-convection. The 2-D simulations were performed at the cross section of the fire front. The simulation domain was set at 85 × 26 km with 110 × 100 grid boxes in the $x$ and $z$ directions. The horizontal grid box size at the center of the $x$ direction was equal to 500 m, and it enlarged towards the lateral boundaries due to the stretched grid (Fig. S1). The vertical grid spacing at the surface and the tropopause was set to 50 and 150 m, respectively. The lowest vertical level in our simulation was placed 766 m above sea level, corresponding to the lowest elevation of the radiosonde data, which is close to the elevation of Chisholm at about 600 m (ASRD, 2001).

The simulations were initialized horizontally homogeneously with radiosonde data from about 200 km south of the fire on 29 May 2001, which is the same as in Luderer (2007) (Fig. S2). Open lateral boundaries were used for the model simulations. The means of wind speed and specific humidity were nudged towards the initial profile at the lateral boundaries. The fire forcing was introduced in the middle grid in the bottom layer of the domain, and its intensity remained constant throughout the simulation of each scenario. Each case was run for 3 simulated hours until the clouds were fully developed and had reached steady state.

### 2.2 Aerosol particles and fire forcing

Atmospheric aerosol particles affect cloud formation through two pathways by acting as CCN and IN. Following the previous study of Reutter et al. (2009), we limited the scope of aerosol-cloud interactions to CCN activation only. So, in this study, changes in $N_{CN}$ do not directly influence frozen hydrometeors by providing IN, but do so indirectly through their impact on CCN activation and subsequent processes.

In this study, 1302 cases ($31 N_{CN} \times 42$ fire forcing values) were simulated to evaluate the interplay of aerosol concentration and updrafts on the formation of clouds and precipitation. The $N_{CN}$ varied from 200 to 100 000 $cm^{-3}$. In each case, $N_{CN}$ was prescribed (distributed uniformly across the modeling domain and kept identical throughout the simulation). A similar treatment and approach has been used in previous studies (Seifert et al., 2012; Reutter et al., 2013). As mentioned above, we used the lookup table of Reutter et al. (2009), which implies the use of their aerosol size distribution as well (log-normal distribution with a geometric mean diameter of 120 nm and a geometric standard deviation of 1.5). For the present study, the aerosol characteristics, such as size distribution, chemical composition, hygroscopicity and mixing state are in fact rather unimportant, compared with the order-of-magnitude changes in the aerosol number concentration (Reutter et al., 2009; Karydis et al., 2012). Therefore, the effects of variations in aerosol characteristics were not considered in our study. In all simulations, clouds were triggered by the fire forcing, which was assumed constant during the simulation. The fire forcing intensity varied from $1 \times 10^3$ to $3 \times 10^5$ $W m^{-2}$. The correlation between the initial fire forcing and corresponding updraft velocity at the cloud base was probed and is described in Sect. 3.1.





ACPD
14, 7777–7822, 2014

## 2.3 Process analysis

Cloud properties are subject to several tens of microphysical processes, e.g., cloud droplet nucleation, autoconversion, freezing, condensation, evaporation, etc. (Seifert and Beheng, 2006). Elevated concentrations of hydrometeors can be caused either by an increase in their sources or by a decrease in their sinks. To improve the understanding of the aerosol-cloud interactions, we employed the process analysis (PA) method to quantify the causation of changes in the concentrations of individual hydrometeor classes.

In addition to the standard model output (e.g., time and spatial series of mass and number concentrations of hydrometeors, and meteorological output), our PA method archives additional parameters, i.e., the time rate of change of hydrometeors due to individual microphysical processes. Table A1 summarizes all the acronyms and their corresponding microphysical processes.

# 3 Results and discussion

## 3.1 Fire forcing and updraft velocity

Fire forcing does not affect the cloud activation of aerosols directly, but it can affect activation indirectly by triggering strong updraft velocities. Updrafts are of importance in the formation of clouds and precipitation for redistributing energy and moisture. In pyro-convective clouds, the updraft velocities range from ca. 0.25 to 20 $\mathrm{m\,s^{-1}}$ (Reutter et al., 2009) and are far greater than the typical magnitudes of updrafts of 1–10 $\mathrm{cm\,s^{-1}}$ (Tonttila et al., 2011).

The probability distribution function of vertical velocities ($w$) at cloud base layer under different fire forcing conditions is shown in Fig. S3a. The velocity on top of the input fire forcing is usually the largest, and decreases towards the lateral sides. As the characteristic velocities, the maximum velocity at cloud base in Fig. S3a, are plotted against the input fire forcing (range of $1\times10^3$ to $3\times10^5\,\mathrm{W\,m^{-2}}$, $N_{\mathrm{CN}} = 1\times10^3\,\mathrm{cm^{-3}}$) in Fig. S3b. The shaded area indicates the variability of estimation over each simulation period. According to the figure, $w$ at cloud base varies monotonically from 1.8 to $27\,\mathrm{m\,s^{-1}}$ as fire forcing increases from $1\times10^3$ to $3\times10^5\,\mathrm{W\,m^{-2}}$. The positive relationship suggests that fire forcing could be a good indicator of vertical velocity.

### 3.2 Sensitivity regimes for hydrometeors and precipitation

In this section, we show the modeled dependency of various hydrometeors on $N_{\mathrm{CN}}$ and fire forcing (FF). Note here only the characteristics of dependency are presented, while the underlying mechanisms will be discussed and interpreted in more detail in Sect. 3.3. For an individual hydrometeor type, the averaged concentrations (over the entire domain and simulation period) were used as metrics in our evaluation, and the condensed water reaching the surface was used as a metric for precipitation.

#### 3.2.1 Cloud droplets

To investigate the sensitivity of an individual hydrometeor to changes in $N_{\mathrm{CN}}$ and FF, we adopted the definition of relative sensitivity $\mathrm{RS}_Y(X)$ (of one variable $Y$ against the variable $X$) as

$$\mathrm{RS}_Y(X) = \frac{\partial Y/Y}{\partial X/X} = \frac{\partial \ln Y}{\partial \ln X} \tag{1}$$

In this study, $X$ is the factor affecting cloud formation, i.e., $N_{\mathrm{CN}}$ and FF, and $Y$ is the mass or number concentration of each hydrometeor type (cloud droplets, raindrops, as well as frozen particles). By using a natural logarithmic calculation of the variables (i.e., $X$, $Y$), the percentage change of an individual parameter relative to its magnitude could be reflected better. This logarithmic sensitivity evaluation has been applied commonly in the assessment of aerosol-cloud interactions (Feingold, 2003; McFiggans





ACPD
14, 7777–7822, 2014

et al., 2006; Kay and Wood, 2008; Reutter et al., 2009; Sorooshian et al., 2009; Karydis et al., 2012).

Figure 2a shows the dependence of cloud water droplets ($N_{CD}$) on $N_{CN}$ and FF. The shape of the isolines is generally consistent with the regime designations reported by Reutter et al. (2009). Following Reutter et al. (2009), a value of the RS($N_{CN}$) to RS(FF) ratio of 4 or 1/4 was taken as the threshold value to distinguish different regimes (the same criteria were employed for rainwater and frozen water content). Red dashed lines in Fig. 2a indicate the borders between different regimes. This resulted in an aerosol-limited regime in the upper left sector of the panel ($N_{CD}$ is sensitive mainly to $N_{CN}$ and is insensitive to fire forcing), an updraft-limited regime in the lower right sector of the panel ($N_{CD}$ displays a linear dependence on FF and a very weak dependence on $N_{CN}$), and the transitional regime along the ridge of the isopleth (FF and $N_{CN}$ play comparable roles in the change of $N_{CD}$). The regimes of Reutter et al. (2009) are derived from simulations of the cloud parcel model of CCN activation at the cloud base. Our results demonstrate that the general regimes for CCN activation still prevail, even when considering full microphysics and the larger temporal and spatial scales of a single pyro-convective cloud system. Figure 2c and 2d demonstrate the changes of normalized number concentrations (relative to the maximum value) as a function of aerosols and fire forcing, respectively. High sensitivities were found for low conditions of $N_{CN}$ and FF. As $N_{CN}$ or FF increases, their impact becomes weaker (Fig. 3a and b). The reduced sensitivity of cloud droplets to aerosols can be explained by the buffering effect of the cloud system, so that the response of the cloud system to aerosols is much smaller than would have been expected had internal interactions not been considered (Stevens and Feingold, 2009).

Compared with $N_{CD}$, the cloud mass concentration ($M_{CD}$) is less sensitive to $N_{CN}$, and there is hardly an aerosol-limited regime in the contour plot for $M_{CD}$ (Figs. 2b and 3c). There are only two regimes indicated by the red dashed line in Fig. 2b: an updraft-limited regime in the lower right sector of the panel, and the transitional regime in the upper sector (an aerosol- and updraft-sensitive regime). The RS($N_{CN}$) of $N_{CD}$ is on





ACPD
14, 7777–7822, 2014

average 10 times higher than that of $M_{CD}$, independent of the intensity of the FF. As $N_{CN}$ increases, $M_{CD}$ becomes insensitive to the change of $N_{CN}$. This strongly suggests that when we evaluate the cloud responses to the changes in the ambient aerosol particles for global models or satellite data, we should focus more on the aerosol effect on cloud droplet number concentration, rather than on the liquid water path. However, the responses of both the normalized $N_{CD}$ and $M_{CD}$ to changes in FF (Fig. 2d and f, respectively) appear similar. Averaged RS(FF) values over simulated FF ranges for $N_{CD}$ (0.60) and $M_{CD}$ (0.50) are commensurate (Fig. 3b and 3d, respectively), which implies that both the number and mass concentrations of cloud droplets are very sensitive to updrafts.

### 3.2.2 Raindrops

The response of the raindrop number concentration ($N_{RD}$) is more complex. When FF is weak ($< 20\,000\,\mathrm{W\,m^{-2}}$), the aerosol effect could be either positive with low $N_{CN}$ ($< 2000\,\mathrm{cm^{-3}}$) or negative with high $N_{CN}$ ($> 2000\,\mathrm{cm^{-3}}$). When FF is strong ($> 20\,000\,\mathrm{W\,m^{-2}}$), $N_{RD}$ decreases monotonically as $N_{CN}$ increases. The effect of FF on $N_{RD}$ is non-monotonic (Figs. 4a and d and 5b). Under low aerosol conditions, FF plays the most positive role at a value of about $6000\,\mathrm{W\,m^{-2}}$, above which the FF effect becomes negative. However, under high aerosol conditions, there are two regions (FF = 3000 and $15\,000\,\mathrm{W\,m^{-2}}$) in which the FF effect is especially significant.

As shown in Fig. 4, FF exhibits positive effects on raindrop formation ($M_{RD}$), whereas the aerosol shows a slightly positive effect with low $N_{CN}$, but a negative effect with large $N_{CN}$. The normalized mass concentrations ($M_{RD}$) relative to the maximum value as a function of aerosols and FF are also displayed in Fig. 4e and f. The influence of FF is much more significant than that of $N_{CN}$ in most cases. For example, the upper left corner (an aerosol-limited regime for $N_{CD}$) becomes a transitional regime for $M_{RD}$ with RS (FF) of 0.1 and RS ($N_{CN}$) of –0.06 (Fig. 5). High RS($N_{CN}$) values of $M_{RD}$ were found at low $N_{CN}$ conditions, and this decreases as $N_{CN}$ increases (Fig. 5c). The $N_{CN}$





ACPD
14, 7777–7822, 2014

exhibits the most negative effects on $M_{RD}$ under intermediate $N_{CN}$ conditions ($N_{CN}$ of several 1000 cm$^{-3}$). In contrast to cloud droplet number concentration, an aerosol-limited regime for $M_{RD}$ hardly exists in our simulations (Fig. 4b). The response of the raindrops to aerosols is much weaker than the response of cloud droplets to aerosols. This finding is consistent with the idea of clouds acting as a buffered system formulated by Stevens and Feingold (2009). However, the feedbacks that were possibly introduced between the cloud macrophysics and microphysics, and the contribution of these two effects (microphysical and macrophysical buffers) still need further investigation.

### 3.2.3 Frozen water contents

Within our microphysical scheme, frozen water contents are grouped into four main classes: ice crystals, snow, graupel, and hail (Seifert and Beheng, 2006). Aerosols exert influence on the frozen water contents via the process of ice nucleation (in), but the processes that convert between the different hydrometeor classes and water vapor play a greater role in changing the concentrations of frozen particles, especially the processes of cloud freezing to form ice (cfi) and the vapor depositional growth of ice and snow (vdi and vds respectively). Figure S4 illustrates the percentage mass contributions of the individual frozen hydrometeor classes to the total frozen mass. The percentages of each hydrometeor are calculated based on average values over the entire simulation period. Generally, greater concentrations of aerosol result in more snow and less graupel. This is in agreement with previous studies on convective clouds (Seifert et al., 2012; Lee and Feingold, 2013), and can be explained by the suppression of the warm rain processes under high aerosol condition. High $N_{CN}$ delays the conversion of the cloud water to form raindrops, so that more cloud water content can ascend to altitudes with sub-zero temperatures, hence freeze into small frozen particles. The percentage of ice crystals does not change much, contributing approximately 20 % on average.

The dependence of total frozen particles on FF and $N_{CN}$ is summarized in Fig. 6. The FF and $N_{CN}$ show positive effects for both the number and mass concentrations of the frozen water particles ($N_{FP}$ and $M_{FP}$, respectively). High RS($N_{CN}$) and RS(FF) values were found at low $N_{CN}$ and FF conditions (Fig. 7), respectively. As $N_{CN}$ or FF increases, their impact becomes weaker, as indicated by a decreasing RS. According to the ratio of RS(FF)/RS($N_{CN}$), both $N_{FP}$ and $M_{FP}$ are within the updraft-limited regime. Again, smaller RS($N_{CN}$) values for $M_{FP}$ compared with $N_{CD}$ illustrate the weaker impact of $N_{CN}$ on the production of frozen particles.

### 3.2.4 Precipitation rate

Surface precipitation rate is a key factor in climate and hydrological processes. Many field measurements, remote sensing studies, and modeling simulations have attempted to evaluate the magnitude of aerosol-induced effects on the surface rainfall rate (Rosenfeld, 1999, 2000; Tao et al., 2007; Li et al., 2008; Sorooshian et al., 2009). The response of averaged surface precipitation rate (over 3 h simulations) to FF and $N_{CN}$ is shown in Fig. 8. The FF has a positive effect on the precipitation, and RS(FF) shows a decreasing trend as FF increases (Fig. 9b).

The effect of $N_{CN}$ is more complex. Both positive and negative RS ($N_{CN}$) were found in our study. There are generally two different regimes: a precipitation-enhanced regime and a precipitation-suppressed regime. In the precipitation-enhanced regime ($N_{CN}$ <∼ 1000 cm$^{-3}$), $N_{CN}$ has a positive effect on the precipitation rate, and increasing $N_{CN}$ will reduce RS ($N_{CN}$) (Fig. 9a). In the precipitation-suppressed regime, aerosols start to reduce the precipitation corresponding to a negative RS($N_{CN}$). Within the precipitation-suppressed regime, there is also an extreme RS($N_{CN}$) at a value of $N_{CN}$ of a few thousand particles per cm$^3$. In the literature, both positive (Tao et al., 2007) and negative effects (Altaratz et al., 2008) of aerosols have been reported in previous case studies. Our simulations suggest that this apparently contradictory phenomenon might be the expression of the same physical processes under different aerosol and dynamic conditions. Regarding the temporal evolution, low $N_{CN}$ results in earlier rainfall (Fig. S5), which is consistent with current understanding, observations (e.g., Rosenfeld, 1999, 2000), and modeling evidence (e.g., the convective cumulus cloud study by

Li et al., 2008). Note that the general relationship between precipitation and aerosols described in this study is based on simulations over a period of 3 h. Simulations for a longer period should be carried out in future studies to investigate the influence of aerosols on precipitation over longer time scales.

## 3.3 Process analysis

The evolution of hydrometeor concentrations is determined by multiple microphysical and dynamical processes. Four extreme cases are taken as examples in the following discussion: (1) LULA, low updrafts (2000 W m$^{-2}$) and low aerosols (200 cm$^{-3}$); (2) LUHA, low updrafts (2000 W m$^{-2}$) and high aerosols (100 000 cm$^{-3}$); (3) HULA, high updrafts (300 000 W m$^{-2}$) and low aerosols (200 cm$^{-3}$); (4) HUHA, high updrafts (300 000 W m$^{-2}$) and high aerosols (100 000 cm$^{-3}$). Here, the LULA, LUHA, HULA, and HUHA cases refer to specific $N_{CN}$/FF values, whereas in Sect. 3.2, they referred to a group of $N_{CN}$/FF conditions.

### 3.3.1 Clouds

Figure 10 shows the temporal evolution of horizontally-averaged $M_{CD}$ under these four pairs of FF and $N_{CN}$ conditions. It is clear that increasing $N_{CN}$ leads to enhanced formation of cloud droplets; stronger updrafts not only result in more $M_{CD}$, but also tend to prolong the lifetime of cloud droplets.

Figure 11 summarizes the microphysical processes that act as the main sources (positive values) and sinks (negative values) for cloud droplets. For $N_{CD}$, the dominant source term is the cloud nucleation (CCN activation) process, in which aerosols are activated under supersaturated water vapor and form cloud droplets. As cloud nucleation happens mostly at the cloud base and so is not strongly affected by cloud dynamical feedbacks, the response of $N_{CD}$ shows similar regimes to cloud parcel models (Reutter et al., 2009). To help explain the regime designation, we divide $N_{CD}$ into two factors: an ambient aerosol number concentration ($N_{CN}$) and an activated fraction ($N_{CD}/N_{CN}$).





ACPD
14, 7777–7822, 2014

Given the aerosol size distributions, the $N_{CD}/N_{CN}$ ratio is determined approximately by the critical activation diameter ($D_c$) above which the aerosols can be activated into cloud droplets. The $D_c$ is a function of ambient supersaturation. Stronger updrafts result in higher supersaturation, smaller $D_c$ and hence, larger $N_{CD}/N_{CN}$ ratios. Under high updraft conditions, $N_{CD}/N_{CN}$ is already close to unity. A further increase in the updraft velocity will still change the supersaturation and $D_c$, but it will not significantly influence the $N_{CD}/N_{CN}$ ratios and $N_{CD}$. In this case, $N_{CD}$ is approximately proportional to $N_{CN}$.

Under weak updrafts, the $N_{CD}/N_{CN}$ ratio is sensitive to ambient supersaturations. In this case, a larger supersaturation induced by stronger updrafts can effectively change the $N_{CD}/N_{CN}$ ratio and thus $N_{CD}$ is sensitive to the updraft velocity. On the other hand, the stronger dependence of $N_{CD}/N_{CN}$ on the supersaturation also changes the role of aerosols. As more aerosols reduce supersaturation, increasing $N_{CN}$ tends to reduce the activated fraction, $N_{CD}/N_{CN}$. Taking $N_{CN} = 60\,000\,\mathrm{cm}^{-3}$ (FF = $2000\,\mathrm{W\,m}^{-2}$), for example, a 10 % increase in $N_{CN}$ causes a 4 % decrease in $N_{CD}/N_{CN}$, whereas a 10 % decrease in $N_{CN}$ leads to an 8 % increase in $N_{CD}/N_{CN}$. The impact of changing $N_{CN}$ on the $N_{CD}/N_{CN}$ ratio counteracts partly or mostly the positive effect of $N_{CN}$ on cloud droplet formation.

The changes of $M_{CD}$ are influenced mainly by the following sources: (1) the condensation of water vapor on the present cloud droplets (vdc) and (2) the cloud nucleation process (cn), and by the following sinks: (3) the autoconversion (au) and (4) the accretion of cloud droplets (ac), and (5) the freezing of cloud droplets to form cloud ice (cfi), which includes heterogeneous (Seifert and Beheng, 2006) and homogeneous freezing processes (Jeffery and Austin, 1997; Cotton and Field, 2002). Concerning their relative contributions, depositional growth of cloud droplets (vdc) is the major source at low aerosol concentrations. As $N_{CN}$ increases, cloud nucleation (cn) becomes more significant and can even outweigh vdc at high aerosol concentrations. The processes of autoconversion (au) and accretion (ac) are the major sinks at weak updrafts. As FF increases, the conversion to frozen particles, especially to ice (the cfi process), becomes increasingly important.

Concerning the absolute contribution, increasing FF enhances the change rate of the conversion of water vapor to the condensed phase ($R_{vdc}$ and $R_{cn}$), whereas increasing $N_{CN}$ tends to reduce it. The FF effect is straightforward and the aerosol effect here is complicated. Aerosols can enhance both the condensation and the evaporation of water vapor from the cloud droplets due to the increase in the surface-to-volume ratio of cloud droplets; condensation increases $M_{CD}$ and evaporation reduces $M_{CD}$. In our study, the net effects are negative (which is expressed in the sign of $\Delta R_{vdc}/\Delta N_{CN}$) and the positive effect of $N_{CN}$ on cn is insufficient to change the overall trend. A similar result has been reported by Khain et al. (2005) for deep convective clouds. They found that high CCN concentrations led to both greater heating and cooling, and that the net convective heating became smaller as CCN increased.

### 3.3.2 Rain

Figure 12 exhibits the temporal evolution of the horizontally-integrated $M_{RD}$. It confirms the result of Fig. 4 that stronger updrafts tend to increase the raindrop concentration, whereas increased aerosol concentration reduces it. This dependence appears simple and similar under different conditions. However, the underlying mechanisms for different scenarios are quite complex.

Dynamic conditions strongly influence the pathways of rain formation and dissipation. For weak updraft cases, rain droplets (e.g., Fig. 13) are produced mainly from autoconversion (au) and accretion (ac), and partly from melted snows (smer) or graupel (gmer). Under this condition, raindrops may appear at altitudes as high as 5–7 km (e.g., Fig. 12a). For high updraft cases, strong updrafts deliver cloud droplets to higher freezing altitudes (Fig. 10). The cloud droplets then turn directly into frozen particles (cloud → ice crystals), without formation of raindrops as an intermediate stage (cloud → rain → larger frozen particles; Fig. 15). Most raindrops are formed from melted frozen droplets and consequently, they appear below ~ 4 km (Fig. 12b). The weaker cloud → rain conversion with higher updrafts also influences the conversion of rain to frozen particles, and is the reason why the rrg process (riming of raindrops to form graupel) under HULA becomes relatively less important than it is under LULA.

The aerosols also modify the pathways of rain formation. Taking weak updraft cases, for example, the accretion process (ac) dominates the cloud → rain conversion under low aerosol concentrations, but is replaced by autoconversion (au) under high aerosol concentrations (Fig. 13). The reason for this is that au is the process that initializes rain formation. Once rain embryos are produced, accretion of cloud droplets by raindrops is triggered and becomes the dominant process of rainwater production, as observed for shallow clouds (Stevens and Seifert, 2008) and stratiform clouds (Wood, 2005). High aerosol loading reduces au, inhibiting the initialization of rain and the following accretion processes at the early stage (0–100 min). In this case, cloud droplets are prone to be converted to ice crystals rather than to raindrops through ac (Figs. 13 and 15). Melted frozen particles are also a major source of raindrops. Under low aerosol concentrations, most of them form from melted graupel particles, whereas under high aerosol concentrations, they are converted mainly from snowflakes. This is consistent with the aerosol impact on the relative abundance of frozen particles shown in Fig. S4. A higher aerosol concentration leads to a higher fraction of smaller frozen particles (ice crystals and snowflakes). The main difference between low and high updrafts is that cloud conversion is the main source in the former case, whereas in the latter case, melted graupel/snow particles become the main contributors.

### 3.3.3 Frozen water content

The time evolutions of frozen water content in Fig. 14 are the manifestations of the aerosol and updraft effects. They confirm the results in Fig. 6 that both $N_{\mathrm{CN}}$ and FF exert positive effects on the generation of frozen particles, and that the influence of FF is the more important factor.

As shown in Fig. 15, the effect of FF is straightforward, boosting vapor deposition (vdi) and cloud droplet freezing on ice (cfi). The vdi is always the most important path-





ACPD
14, 7777–7822, 2014

Aerosol and dynamic effects on the formation of pyro-clouds

D. Chang et al.

way for the formation of frozen particles in our simulations, whereas riming of raindrops to form graupel (rrg) and cfi show comparable contributions in the LULA and HULA cases, respectively. Over a wide range of aerosol concentrations and updraft velocities, our results have extended and generalized the results of Yin et al. (2005), in which vdi and cfi were suggested as the dominant processes controlling the formation of ice crystals in individual mixed-phase convective clouds. Although snow is the dominant constituent of frozen particle mass (Fig. S4), the deposition of vapor on ice (vdi) rather than on snow is the major pathway for frozen particles. The increase of snow mass is mostly caused by collecting of ice (ics) and ice self-collection (coagulation of ice particles, iscs), which are internal conversions not counted as either a source or a sink of frozen water content. Increasing FF enhances the upward transport of water vapor and liquid water to higher altitudes where frozen particles can be formed effectively through vdi and cfi. On the other hand, stronger FF reduces the residence time of cloud droplets in the warm environment (to form raindrops), which could explain the attenuation of rrg in the HULA case.

Positive effects of aerosols on the frozen water content have been demonstrated in Sect. 3.2.4. As shown in Fig. 15, such positive effects are achieved through the enhancement of the vdi process. The depositional growth rate $R_{\mathrm{vdi}}$ is a function of the number concentration ($N_{\mathrm{ice}}$) and size ($D_{\mathrm{ice}}$) of ice, together with the ambient supersaturation over ice ($S_{\mathrm{ice}}$). In our simulations, the averaged $S_{\mathrm{ice}}$ and $D_{\mathrm{ice}}$ are not sensitive to the aerosol disturbance; it is the $N_{\mathrm{ice}}$ that has been increased significantly because of elevated aerosol concentrations. Higher $N_{\mathrm{ice}}$ provides a larger surface area for water vapor deposition on the existing ice crystals and increases $R_{\mathrm{vdi}}$. Lee and Penner (2010) have suggested similar mechanisms for cirrus clouds.



ACPD
14, 7777–7822, 2014

Aerosol and dynamic effects on the formation of pyro-clouds

D. Chang et al.

# 4 Conclusions

In this study, the roles of fire forcing (FF, which triggers updraft velocities) and aerosol number concentration ($N_{CN}$) on the formation and evolution of pyro-convective clouds have been studied in detail and the results are summarized as follows:

1. Both increasing aerosols and FF enhanced the formation of cloud droplets. There are three distinct regimes for the cloud number concentration: an updraft-limited regime (high RS(FF)/RS($N_{CN}$) ratio), an aerosol-limited regime (low RS(FF)/RS($N_{CN}$) ratio), and a transitional regime (intermediate RS(FF)/RS($N_{CN}$) ratio), which agrees well with the regimes derived from a parcel model (Reutter et al., 2009). The cloud mass concentration is less sensitive to aerosols, and there are two regimes for mass concentration: an updraft-limited regime, and a transitional regime.

2. The production of rain water content (i.e., $M_{RD}$) was positively correlated with updrafts, and the aerosol effect could be either slightly positive with low $N_{CN}$ or negative with large $N_{CN}$. The $N_{CN}$ had mostly negative effects on $M_{CD}$ under intermediate $N_{CN}$ conditions ($N_{CN}$ of several 1000 cm$^{-3}$). $M_{RD}$ was generally within an updraft-limited regime, i.e., $M_{RD}$ was very sensitive to changes in updrafts, but insensitive to aerosol concentrations (RS(FF)/RS($N_{CN}$) > 4). The aerosol and FF effects on raindrop number concentrations ($N_{RD}$) are quite complicated; both of them could have either positive or negative effects on the $N_{RD}$.

3. Both updrafts and aerosols showed positive effects on the domain-averaged number and mass concentrations of frozen particles ($N_{FP}$ and $M_{FP}$ respectively). $N_{FP}$ and $M_{FP}$ were also within the updraft-limited regime, which is characterized by large RS(FF)/RS($N_{CN}$) ratio. In this regime, $N_{FP}$ and $M_{FP}$ were directly proportional to fire forcing, and independent of aerosols.

4. Larger FF resulted in more precipitation, whereas the effect of aerosols on precipitation was complex and could be either positive or negative.





ACPD
14, 7777–7822, 2014



Title Page
Abstract Introduction
Conclusions References
Tables Figures
◂ ▸
Back Close
Full Screen / Esc
Printer-friendly Version
Interactive Discussion

5. In addition, when $N_{CN}$ and FF became too large, their impact became weaker, as indicated by a decreasing RS.

The PA provided further insight into the mechanisms of aerosol-cloud interactions. By evaluating the contribution of the relevant microphysical processes to the formation of an individual hydrometeor, the PA revealed the dominant factors responsible for the changes in hydrometeor number and mass. (1) Cloud nucleation (cn) initializes cloud droplet formation and is the major factor that controls the number concentration of cloud droplets. As expected, the increase in cloud droplet mass can be attributed mostly to the condensational growth (vdc). (2) Under weak FF, autoconversion (au) and accretion (ac) are the main sources of rain droplets. Under strong FF, the major source is the melting of frozen particles. (3) For the frozen content, water vapor deposition on existing ice crystals (vdi) is the most important contributor. In addition to CCN activation, the PA also highlights the importance of other microphysical processes in regulating cloud evolution, which is worthy of further scrutiny.

While the general trend is clear, the inclusion of nonlinear (dynamic and microphysical) processes leads to a complex and unstable response of clouds to aerosol perturbations. This applies to the response of all hydrometeors and precipitation, as indicated by the large standard deviation of RS in Figs. 3, 5, and 7. This should also hold when variations in other parameters (e.g., meteorological conditions) are introduced. Compared with our results, the RS derived from cloud parcel modeling is much smoother (Fig. 8 in Reutter et al., 2009). The difference is probably caused by complex interactions between cloud microphysics and dynamics (Khain et al., 2008; Fan et al., 2009). These highly nonlinear processes result in a more unstable and chaotic response of cloud evolution to aerosol and dynamic perturbations. Because of this non-linearity, sensitivities of clouds based on limited case studies may require caveats, because they may not be as representative as expected, and so cannot safely be extrapolated to conditions outside of the range explored. To understand better the role of aerosols in cloud formation, we recommend high-resolution ensemble sensitivity studies over a wide range of dynamic and aerosol conditions.





ACPD
14, 7777–7822, 2014

General current understanding and global modelling studies suggest that for cloud droplet number concentration, the updraft-limited regime may be more characteristic of continental clouds, while the aerosol-limited regime may be more characteristic of marine clouds (e.g., Karydis et al., 2012), suggesting that aerosol effects are generally more important for the marine environment. For this case study, then, we conclude that aerosol effects on cloud droplet number concentrations and thus cloud radiative properties (first indirect effect) are likely more important than effects on precipitation and thus cloud lifetime (second indirect effect), since precipitation is far less sensitive to aerosol number concentrations than to updraft velocity. This is in agreement with other studies (e.g., Seifert et al., 2012). However, it must still be determined whether this conclusion applies to other cloud types and over longer time scales.

In future work, we intend to extend the current studies to: (1) include other types of clouds with other meteorological or atmospheric conditions; (2) investigate the cloud response over longer timescales, as different observational scales could introduce biases in the quantification of aerosol effects on clouds (McComiskey and Feingold, 2012); and (3) evaluate the relative contribution of microphysical and dynamic effects to cloud buffering effects (Stevens and Feingold, 2009; Seifert et al., 2012).

**Supplementary material related to this article is available online at http://www.atmos-chem-phys-discuss.net/14/7777/2014/acpd-14-7777-2014-supplement.pdf.**

*Acknowledgements.* This work was supported by the Max Planck Society (MPG), Max Planck Graduate Center (MPGC), and EU project BACCHUS (No. 603445). Susannah Burrows was supported by the Office of Science Biological and Environmental Research Program of the US Department of Energy as part of the Earth System Modelling Program. We thank A. Seifert, P. Spichtinger and P. Neis for helpful discussions and model setup.

The service charges for this open access publication
have been covered by the Max Planck Society.

## References

Ackerman, A. S., Toon, O. B., Stevens, D. E., Heymsfield, A. J., Ramanathan, V., and Welton, E. J.: Reduction of tropical cloudiness by soot, Science, 288, 1042–1047, doi:10.1126/science.288.5468.1042, 2000.

Ackerman, A. S., Toon, O. B., Stevens, D. E., and Coakley, J. A.: Enhancement of cloud cover and suppression of nocturnal drizzle in stratocumulus polluted by haze, Geophys. Res. Lett., 30, 1381, doi:10.1029/2002gl016634, 2003.

Ackerman, A. S., Kirkpatrick, M. P., Stevens, D. E., and Toon, O. B.: The impact of humidity above stratiform clouds on indirect aerosol climate forcing, Nature, 432, 1014–1017, doi:10.1038/Nature03174, 2004.

Albrecht, B. A.: Aerosols, cloud microphysics, and fractional cloudiness, Science, 245, 1227–1230, doi:10.1126/science.245.4923.1227, 1989.

Altaratz, O., Koren, I., Reisin, T., Kostinski, A., Feingold, G., Levin, Z., and Yin, Y.: Aerosols' influence on the interplay between condensation, evaporation and rain in warm cumulus cloud, Atmos. Chem. Phys., 8, 15–24, doi:10.5194/acp-8-15-2008, 2008.

Andreae, M. O., Rosenfeld, D., Artaxo, P., Costa, A. A., Frank, G. P., Longo, K. M., and Silva-Dias, M. A. F.: Smoking rain clouds over the Amazon, Science, 303, 1337–1342, 2004.

ASRD: Final documentation report-Chisholm Fire (LWF-063), Forest Protection Division, ISBN 0-7785-1841-8, Tech. Rep., Sustainable Resource Development, Alberta, 2001.

Bell, T. L., Rosenfeld, D., Kim, K. M., Yoo, J. M., Lee, M. I., and Hahnenberger, M.: Midweek increase in US summer rain and storm heights suggests air pollution invigorates rainstorms, J. Geophys. Res.-Atmos., 113, D02209, doi:10.1029/2007jd008623, 2008.

Blahak, U.: Towards a Better Representation of High Density Ice Particles in a State-of-the-Art Two-Moment Bulk Microphysical Scheme, 15th International Conf. on Clouds and Precipitation, Cancun, Mexico, 2008.

Carslaw, K. S., Lee, L. A., Reddington, C. L., Pringle, K. J., Rap, A., Forster, P. M., Mann, G. W., Spracklen, D. V., Woodhouse, M. T., Regayre, L. A., and Pierce, J. R.: Large contribution of natural aerosols to uncertainty in indirect forcing, Nature, 503, 67–71, doi:10.1038/Nature12674, 2013.

Conant, W. C., VanReken, T. M., Rissman, T. A., Varutbangkul, V., Jonsson, H. H., Nenes, A., Jimenez, J. L., Delia, A. E., Bahreini, R., Roberts, G. C., Flagan, R. C., and Seinfeld, J. H.:





ACPD
14, 7777–7822, 2014

Aerosol-cloud drop concentration closure in warm cumulus, J. Geophys. Res.-Atmos., 109, D13204, doi:10.1029/2003jd004324, 2004.
Cotton, R. J. and Field, P. R.: Ice nucleation characteristics of an isolated wave cloud, Q. J. Roy. Meteor. Soc., 128, 2417–2437, doi:10.1256/Qj.01.150, 2002.
Fan, J. W., Yuan, T. L., Comstock, J. M., Ghan, S., Khain, A., Leung, L. R., Li, Z. Q., Martins, V. J., and Ovchinnikov, M.: Dominant role by vertical wind shear in regulating aerosol effects on deep convective clouds, J. Geophys. Res.-Atmos., 114, D22206, doi:10.1029/2009jd012352, 2009.
Feingold, G.: Modeling of the first indirect effect: analysis of measurement requirements, Geophys. Res. Lett., 30, 1997, doi:10.1029/2003gl017967, 2003.
Fountoukis, C., Nenes, A., Meskhidze, N., Bahreini, R., Conant, W. C., Jonsson, H., Murphy, S., Sorooshian, A., Varutbangkul, V., Brechtel, F., Flagan, R. C., and Seinfeld, J. H.: Aerosol-cloud drop concentration closure for clouds sampled during the International Consortium for Atmospheric Research on Transport and Transformation 2004 campaign, J. Geophys. Res.-Atmos., 112, D10S30, doi:10.1029/2006jd007272, 2007.
Fromm, M., Shettle, E. P., Fricke, K. H., Ritter, C., Trickl, T., Giehl, H., Gerding, M., Barnes, J. E., O'Neill, M., Massie, S. T., Blum, U., McDermid, I. S., Leblanc, T., and Deshler, T.: Stratospheric impact of the Chisholm pyrocumulonimbus eruption: 2. Vertical profile perspective, J. Geophys. Res.-Atmos., 113, D08203, doi:10.1029/2007jd009147, 2008.
Graf, H. F., Herzog, M., Oberhuber, J. M., and Textor, C.: Effect of environmental conditions on volcanic plume rise, J. Geophys. Res.-Atmos., 104, 24309–24320, 1999.
Grandey, B. S., Stier, P., and Wagner, T. M.: Investigating relationships between aerosol optical depth and cloud fraction using satellite, aerosol reanalysis and general circulation model data, Atmos. Chem. Phys., 13, 3177–3184, doi:10.5194/acp-13-3177-2013, 2013.
Gunthe, S. S., Rose, D., Su, H., Garland, R. M., Achtert, P., Nowak, A., Wiedensohler, A., Kuwata, M., Takegawa, N., Kondo, Y., Hu, M., Shao, M., Zhu, T., Andreae, M. O., and Pöschl, U.: Cloud condensation nuclei (CCN) from fresh and aged air pollution in the megacity region of Beijing, Atmos. Chem. Phys., 11, 11023–11039, doi:10.5194/acp-11-11023-2011, 2011.
Herzog, M.: Simulation der dynamik eines multikomponentensystems am beispiel vulkanischer eruptionswolken, Ph.D., University of Hamburg, Hamburg, Germany, 153 pp., 1998.
Herzog, M., Graf, H. F., Textor, C., and Oberhuber, J. M.: The effect of phase changes of water on the development of volcanic plumes, J. Volcanol. Geoth. Res., 87, 55–74, 1998.

Herzog, M., Oberhuber, J. M., and Graf, H. F.: A prognostic turbulence scheme for the nonhydrostatic plume model ATHAM, J. Atmos. Sci., 60, 2783–2796, 2003.

Hobbs, P. V. and Locatelli, J. D.: Ice nuclei from a natural forest fire, J. Appl. Meteorol., 8, 833–834, 1969.

Hobbs, P. V. and Radke, L. F.: Cloud Condensation Nuclei from a Simulated Forest Fire, Science, 163, 279–280, 1969.

IPCC: Climate change 2007: The physical science basis, Contribution of Working Group I to the Fourth Assessment Report of the Intergovernmental Panel on Climate Change, edited by: Solomon, S., Qin, D., Manning, M., Chen, Z., Marquis, M., Averyt, K. B., Tignor, M., and Miller, H. L., Cambridge University Press, Cambridge and New York, 2007.

Jeffery, C. A. and Austin, P. H.: Homogeneous nucleation of supercooled water: results from a new equation of state, J. Geophys. Res.-Atmos., 102, 25269–25279, doi:10.1029/97jd02243, 1997.

Karydis, V. A., Capps, S. L., Russell, A. G., and Nenes, A.: Adjoint sensitivity of global cloud droplet number to aerosol and dynamical parameters, Atmos. Chem. Phys., 12, 9041–9055, doi:10.5194/acp-12-9041-2012, 2012.

Kaufman, Y. J. and Fraser, R. S.: The effect of smoke particles on clouds and climate forcing, Science, 277, 1636–1639, 1997.

Kaufman, Y. J. and Koren, I.: Smoke and pollution aerosol effect on cloud cover, Science, 313, 655–658, doi:10.1126/science.1126232, 2006.

Kaufman, Y. J., Tanre, D., and Boucher, O.: A satellite view of aerosols in the climate system, Nature, 419, 215–223, doi:10.1038/Nature01091, 2002.

Kay, J. E. and Wood, R.: Timescale analysis of aerosol sensitivity during homogeneous freezing and implications for upper tropospheric water vapor budgets, Geophys. Res. Lett., 35, doi:10.1029/2007gl032628, 2008.

Khain, A., Rosenfeld, D., and Pokrovsky, A.: Aerosol impact on the dynamics and microphysics of deep convective clouds, Q. J. Roy. Meteor. Soc., 131, 2639–2663, doi:10.1256/Qj.04.62, 2005.

Khain, A. P., BenMoshe, N., and Pokrovsky, A.: Factors determining the impact of aerosols on surface precipitation from clouds: an attempt at classification, J. Atmos. Sci., 65, 1721–1748, doi:10.1175/2007jas2515.1, 2008.

Kohler, H.: The nucleus in and the growth of hygroscopic droplets., T. Faraday Soc., 32, 1152–1161, doi:10.1039/Tf9363201152, 1936.

Koren, I., Kaufman, Y. J., Remer, L. A., and Martins, J. V.: Measurement of the effect of Amazon smoke on inhibition of cloud formation, Science, 303, 1342–1345, doi:10.1126/science.1089424, 2004.

Kulmala, M., Laaksonen, A., Charlson, R. J., and Korhonen, P.: Clouds without supersaturation, Nature, 388, 336–337, doi:10.1038/41000, 1997.

Laaksonen, A., Korhonen, P., Kulmala, M., and Charlson, R. J.: Modification of the Kohler equation to include soluble trace gases and slightly soluble substances, J. Atmos. Sci., 55, 853–862, 1998.

Lee, S. S. and Penner, J. E.: Aerosol effects on ice clouds: can the traditional concept of aerosol indirect effects be applied to aerosol-cloud interactions in cirrus clouds?, Atmos. Chem. Phys., 10, 10345–10358, doi:10.5194/acp-10-10345-2010, 2010.

Lee, S.-S. and Feingold, G.: Aerosol effects on the cloud-field properties of tropical convective clouds, Atmos. Chem. Phys., 13, 6713–6726, doi:10.5194/acp-13-6713-2013, 2013.

Levin, Z. and Cotton, W.: Aerosol Pollution Impact on Precipitation: a Scientific Review, World Meteorol. Organ., Geneva, Switzerland, 2007.

Li, G. H., Wang, Y., and Zhang, R. Y.: Implementation of a two-moment bulk microphysics scheme to the WRF model to investigate aerosol-cloud interaction, J. Geophys. Res.-Atmos., 113, D15211, doi:10.1029/2007jd009361, 2008.

Lin, J. C., Matsui, T., Pielke, R. A., and Kummerow, C.: Effects of biomass-burning-derived aerosols on precipitation and clouds in the Amazon Basin: a satellite-based empirical study, J. Geophys. Res.-Atmos., 111, D19204, doi:10.1029/2005jd006884, 2006.

Liu, X. H., Zhang, Y., Xing, J., Zhang, Q. A., Wang, K., Streets, D. G., Jang, C., Wang, W. X., and Hao, J. M.: Understanding of regional air pollution over China using CMAQ, Part II. Process analysis and sensitivity of ozone and particulate matter to precursor emissions, Atmos. Environ., 44, 3719–3727, doi:10.1016/j.atmosenv.2010.03.036, 2010.

Luderer, G., Trentmann, J., Winterrath, T., Textor, C., Herzog, M., Graf, H. F., and Andreae, M. O.: Modeling of biomass smoke injection into the lower stratosphere by a large forest fire (Part II): sensitivity studies, Atmos. Chem. Phys., 6, 5261–5277, doi:10.5194/acp-6-5261-2006, 2006.

Luderer, G. G.: Modeling of Deep-Convective Vertical Transport of Foreset Fire Smoke into the Upper Troposphere and Lower Stratosphere, Ph.D., Physics Department, Johannes Gutenberg University Mainz, Mainz, 2007.

McComiskey, A., and Feingold, G.: The scale problem in quantifying aerosol indirect effects, Atmos. Chem. Phys., 12, 1031–1049, doi:10.5194/acp-12-1031-2012, 2012.
McFiggans, G., Artaxo, P., Baltensperger, U., Coe, H., Facchini, M. C., Feingold, G., Fuzzi, S., Gysel, M., Laaksonen, A., Lohmann, U., Mentel, T. F., Murphy, D. M., O'Dowd, C. D., Snider, J. R., and Weingartner, E.: The effect of physical and chemical aerosol properties on warm cloud droplet activation, Atmos. Chem. Phys., 6, 2593–2649, 2006, http://www.atmos-chem-phys.net/6/2593/2006/.
Norris, J. R.: Has northern Indian Ocean cloud cover changed due to increasing anthropogenic aerosol?, Geophys. Res. Lett., 28, 3271–3274, doi:10.1029/2001gl013547, 2001.
Oberhuber, J. M., Herzog, M., Graf, H. F., and Schwanke, K.: Volcanic plume simulation on large scales, J. Volcanol. Geoth. Res., 87, 29–53, 1998.
Petters, M. D. and Kreidenweis, S. M.: A single parameter representation of hygroscopic growth and cloud condensation nucleus activity, Atmos. Chem. Phys., 7, 1961–1971, 2007, http://www.atmos-chem-phys.net/7/1961/2007/.
Pruppacher, H. R. and Klett, J. D.: Microphysics of Clouds and Precipitation, 2nd edn. with an Introduction to Cloud Chemistry and Cloud Electricity, Kluwer Academic Publishers, Reidel, Dordrecht, 954 pp., 1997.
Qian, Y., Gong, D. Y., Fan, J. W., Leung, L. R., Bennartz, R., Chen, D. L., and Wang, W. G.: Heavy pollution suppresses light rain in China: observations and modeling, J. Geophys. Res.-Atmos., 114, D00K02, doi:10.1029/2008jd011575, 2009.
Reid, J. S., Koppmann, R., Eck, T. F., and Eleuterio, D. P.: A review of biomass burning emissions part II: intensive physical properties of biomass burning particles, Atmos. Chem. Phys., 5, 799–825, doi:10.5194/acp-5-799-2005, 2005.
Reutter, P., Su, H., Trentmann, J., Simmel, M., Rose, D., Gunthe, S. S., Wernli, H., Andreae, M. O., and Pöschl, U.: Aerosol- and updraft-limited regimes of cloud droplet formation: influence of particle number, size and hygroscopicity on the activation of cloud condensation nuclei (CCN), Atmos. Chem. Phys., 9, 7067–7080, doi:10.5194/acp-9-7067-2009, 2009.
Reutter, P., Trentmann, J., Seifert, A., Neis, P., Su, H., Herzog, M., Wernli, H., Andreae, M. O., and Pöschl, U.: 3-D model simulations of dynamical and microphysical interactions in pyroconvective clouds under idealized conditions, Atmos. Chem. Phys. Discuss., 13, 19527–19557, doi:10.5194/acpd-13-19527-2013, 2013.
Rosenfeld, D.: TRMM observed first direct evidence of smoke from forest fires inhibiting rainfall, Geophys. Res. Lett., 26, 3105–3108, 1999.

Rosenfeld, D.: Suppression of rain and snow by urban and industrial air pollution, Science, 287, 1793–1796, 2000.
Rosenfeld, D., Fromm, M., Trentmann, J., Luderer, G., Andreae, M. O., and Servranckx, R.: The Chisholm firestorm: observed microstructure, precipitation and lightning activity of a pyro-cumulonimbus, Atmos. Chem. Phys., 7, 645–659, doi:10.5194/acp-7-645-2007, 2007.
Rosenfeld, D., Lohmann, U., Raga, G. B., O'Dowd, C. D., Kulmala, M., Fuzzi, S., Reissell, A., and Andreae, M. O.: Flood or drought: how do aerosols affect precipitation?, Science, 321, 1309–1313, doi:10.1126/science.1160606, 2008.
Saleeby, S. M., Cotton, W. R., Lowenthal, D., Borys, R. D., and Wetzel, M. A.: Influence of cloud condensation nuclei on orographic snowfall, J. Appl. Meteorol. Clim., 48, 903–922, doi:10.1175/2008jamc1989.1, 2009.
Sassen, K. and Khvorostyanov, V. I.: Cloud effects from boreal forest fire smoke: evidence for ice nucleation from polarization lidar data and cloud model simulations, Environ. Res. Lett., 3, 025006, doi:10.1088/1748-9326/3/2/025006, 2008.
Seifert, A. and Beheng, K. D.: A two-moment cloud microphysics parameterization for mixed-phase clouds. Part 1: Model description, Meteorol. Atmos. Phys., 92, 45–66, doi:10.1007/s00703-005-0112-4, 2006.
Seifert, A., Khain, A., Pokrovsky, A., and Beheng, K. D.: A comparison of spectral bin and two-moment bulk mixed-phase cloud microphysics, Atmos. Res., 80, 46–66, doi:10.1016/j.atmosres.2005.06.009, 2006.
Seifert, A., Köhler, C., and Beheng, K. D.: Aerosol-cloud-precipitation effects over Germany as simulated by a convective-scale numerical weather prediction model, Atmos. Chem. Phys., 12, 709–725, doi:10.5194/acp-12-709-2012, 2012.
Shulman, M. L., Jacobson, M. C., Charlson, R. J., Synovec, R. E., and Young, T. E.: Dissolution behavior and surface tension effects of organic compounds in nucleating cloud droplets, Geophys. Res. Lett., 23, 603–603, doi:10.1029/96gl00594, 1996.
Sorooshian, A., Feingold, G., Lebsock, M. D., Jiang, H. L., and Stephens, G. L.: On the precipitation susceptibility of clouds to aerosol perturbations, Geophys. Res. Lett., 36, L13803, doi:10.1029/2009gl038993, 2009.
Stevens, B.: Climate Science: uncertain then, irrelevant now, Nature, 503, 47–48, 2013.
Stevens, B. and Feingold, G.: Untangling aerosol effects on clouds and precipitation in a buffered system, Nature, 461, 607–613, doi:10.1038/Nature08281, 2009.





ACPD
14, 7777–7822, 2014

Stevens, B. and Seifert, A.: Understanding macrophysical outcomes of microphysical choices in simulations of shallow cumulus convection, J. Meteorol. Soc. Jpn., 86, 143–162, 2008.
Su, H., Rose, D., Cheng, Y. F., Gunthe, S. S., Massling, A., Stock, M., Wiedensohler, A., Andreae, M. O., and Pöschl, U.: Hygroscopicity distribution concept for measurement data analysis and modeling of aerosol particle mixing state with regard to hygroscopic growth and CCN activation, Atmos. Chem. Phys., 10, 7489–7503, doi:10.5194/acp-10-7489-2010, 2010.
Tao, W. K., Li, X. W., Khain, A., Matsui, T., Lang, S., and Simpson, J.: Role of atmospheric aerosol concentration on deep convective precipitation: cloud-resolving model simulations, J. Geophys. Res.-Atmos., 112, D24S18, doi:10.1029/2007jd008728, 2007.
Tessendorf, S. A., Weeks, C. E., Axisa, D., and Bruintjes, R. T.: Aerosol characteristics observed in southeast Queensland and implications for cloud microphysics, J. Geophys. Res.-Atmos., 118, 2858–2871, doi:10.1002/Jgrd.50274, 2013.
Tonse, S. R., Brown, N. J., Harley, R. A., and Jinc, L.: A process-analysis based study of the ozone weekend effect, Atmos. Environ., 42, 7728–7736, doi:10.1016/j.atmosenv.2008.05.061, 2008.
Tonttila, J., O'Connor, E. J., Niemelä, S., Räisänen, P., and Järvinen, H.: Cloud base vertical velocity statistics: a comparison between an atmospheric mesoscale model and remote sensing observations, Atmos. Chem. Phys., 11, 9207–9218, doi:10.5194/acp-11-9207-2011, 2011.
Trentmann, J., Luderer, G., Winterrath, T., Fromm, M. D., Servranckx, R., Textor, C., Herzog, M., Graf, H. F., and Andreae, M. O.: Modeling of biomass smoke injection into the lower stratosphere by a large forest fire (Part I): reference simulation, Atmos. Chem. Phys., 6, 5247–5260, 2006,
http://www.atmos-chem-phys.net/6/5247/2006/.
Williams, E., Rosenfeld, D., Madden, N., Gerlach, J., Gears, N., Atkinson, L., Dunnemann, N., Frostrom, G., Antonio, M., Biazon, B., Camargo, R., Franca, H., Gomes, A., Lima, M., Machado, R., Manhaes, S., Nachtigall, L., Piva, H., Quintiliano, W., Machado, L., Artaxo, P., Roberts, G., Renno, N., Blakeslee, R., Bailey, J., Boccippio, D., Betts, A., Wolff, D., Roy, B., Halverson, J., Rickenbach, T., Fuentes, J., and Avelino, E.: Contrasting convective regimes over the Amazon: implications for cloud electrification, J. Geophys. Res.-Atmos., 107, 8082, doi:10.1029/2001jd000380, 2002.
Wood, R.: Drizzle in stratiform boundary layer clouds, Part II: Microphysical aspects, J. Atmos. Sci., 62, 3034–3050, doi:10.1175/Jas3530.1, 2005.

Yin, Y., Carslaw, K. S., and Feingold, G.: Vertical transport and processing of aerosols in a mixed-phase convective cloud and the feedback on cloud development, Q. J. Roy. Meteor. Soc., 131, 221–245, doi:10.1256/qj.03.186, 2005.

Yu, S. C., Mathur, R., Kang, D. W., Schere, K., and Tong, D.: A study of the ozone formation by ensemble back trajectory-process analysis using the Eta-CMAQ forecast model over the northeastern US during the 2004 ICARTT period, Atmos. Environ., 43, 355–363, doi:10.1016/j.atmosenv.2008.09.079, 2009.





ACPD

14, 7777–7822, 2014

**Table A1.** Symbols and acronyms for individual microphysical process.

| Symbol | Process |
|---|---|
| crg/$h$ | Riming of cloud droplets to form graupel/hail |
| cri/$s$ | Riming of cloud droplets to form ice crystals/snow |
| cfi* | Freezing of cloud water to form ice crystals |
| imc | Melting of ice crystals to form cloud water |
| au | Autoconversion of cloud water to form rain |
| ac | Accretion of cloud water by rain |
| cn | Cloud nucleation |
| in | Ice nucleation |
| $g$/hmi | Graupel/hail multiplication to form ice crystals |
| rsc | Self-collection of raindrops |
| imcr | Melting of ice crystals to form cloud water and rain |
| icg | Conversion of ice crystals to form graupel |
| rri/$g$/$h$ | Riming of rain to form ice crystals/graupel/hail |
| irg | Riming of ice crystals to form graupel |
| smi | Snow multiplication to form ice crystals |
| vdc/$i$/$g$/$s$ | Depositional growth of cloud droplets/ice crystals/graupel/snow |
| rfi/$g$/$h$ | Freezing of rain drops to form ice crystals/graupel/hail |
| iscs | Self-collection of ice crystals to form snow |
| iclg/$h$/$s$ | Collection of ice crystals to form graupel/hail/snow |
| $g$/$h$/$s$/imer | Melting of graupel/hail/snow/ice to form raindrops |
| gsr | Shedding of graupel to form raindrops |
| $r$/gep | Evaporation of rain/graupel |
| scg | Conversion of snow to form graupel |

* Here, cfi process includes both heterogeneous and homogeneous freezing processes.





ACPD
14, 7777–7822, 2014

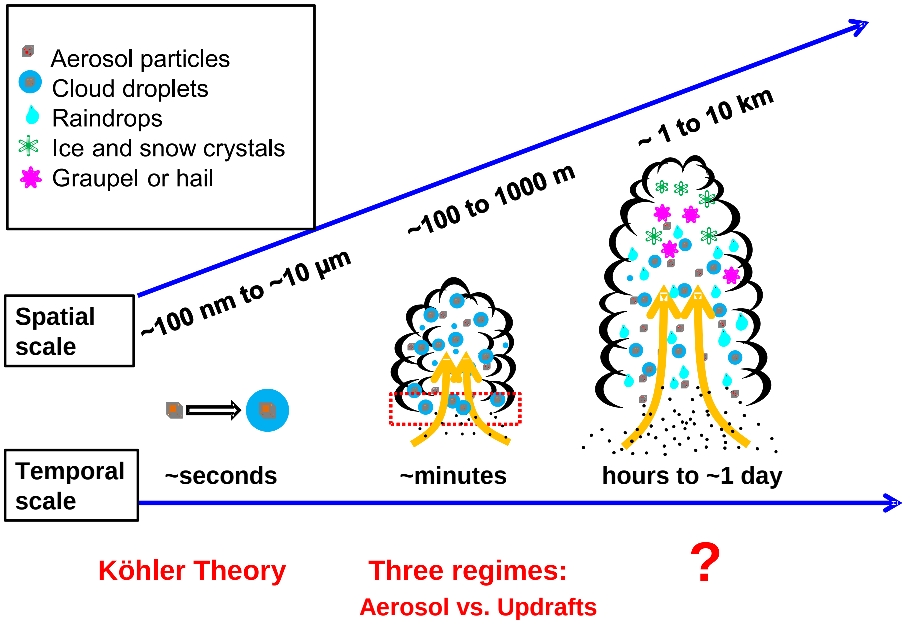


**Fig. 1.** Overview of the research approaches on multi-scale cloud initialization and development.





ACPD
14, 7777–7822, 2014

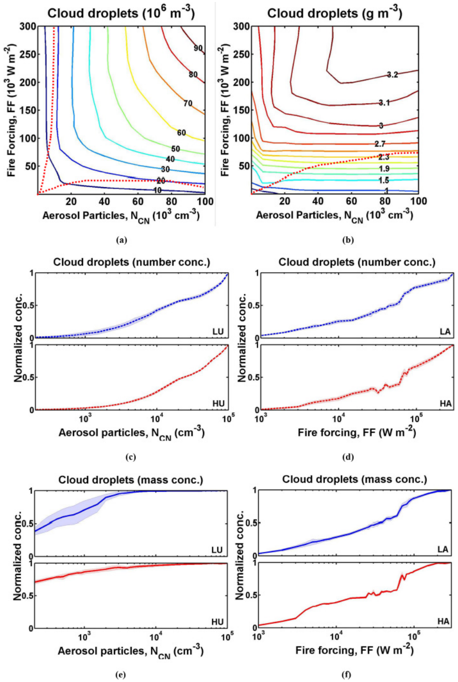


**Fig. 2.** Number **(a)** and mass concentration **(b)** of cloud droplets calculated as a function of aerosol number concentration ($N_{CN}$) and updraft velocity (represented by FF). Red dashed lines indicate the borders between different regimes defined by RS ($N_{CN}$)/RS(FF) = 4 or 1/4, respectively. Normalized cloud droplet number concentration (relative to the maximum value) as a function of $N_{CN}$ **(c)** and FF **(d)**; and normalized mass concentrations as a function of $N_{CN}$ **(e)** and FF **(f)**. The thick dashed or solid lines represent the mean values under a given condition, and the shaded areas represent the variability of estimation ($\pm 1/2\sigma$). The acronyms indicate LU: low updrafts (1000–7000 W m$^{-2}$); HU: high updrafts (75 000–300 000 W m$^{-2}$); LA: low aerosols (200–1500 cm$^{-3}$); HA: high aerosols (10 000–100 000 cm$^{-3}$).





ACPD
14, 7777–7822, 2014



D. Chang et al.

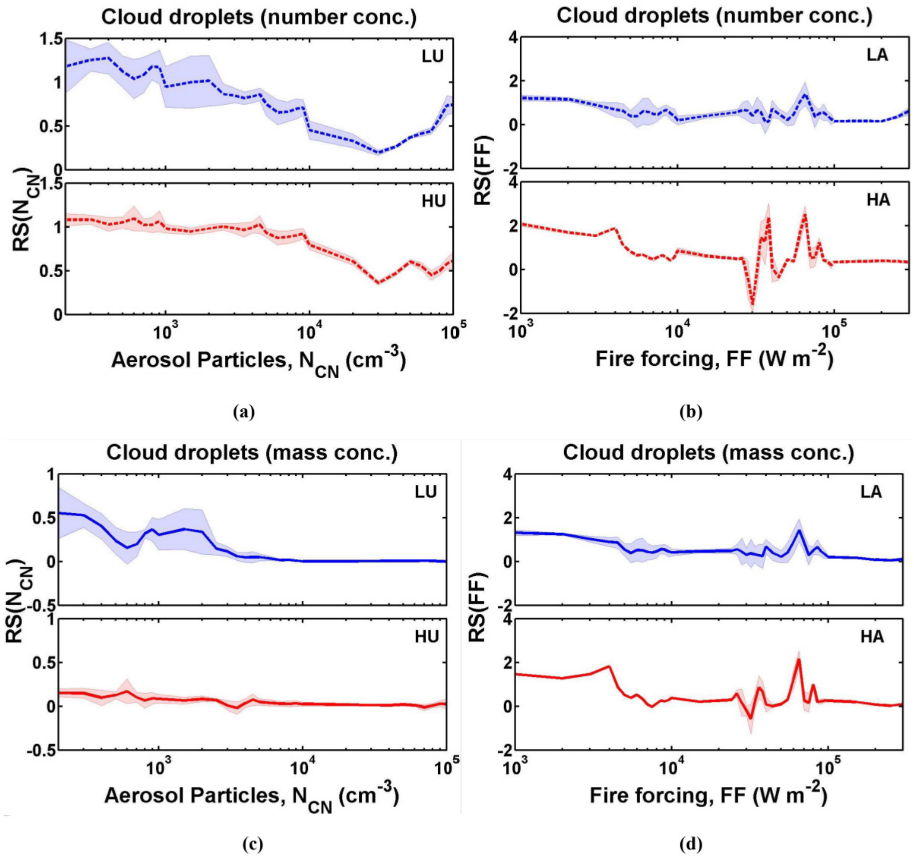


**Fig. 3.** Relative sensitivities with respect to $N_{CN}$ (left) and FF (right) for number (**a** and **b**) and mass (**c** and **d**) concentration of cloud droplets under different conditions. The meaning of the acronyms (LU, HU, LA, HA) is the same as that in Fig. 2. The shaded areas represent the variability of estimation ($\pm 1/2\sigma$).





ACPD
14, 7777–7822, 2014

Aerosol and dynamic effects on the formation of pyro-clouds

D. Chang et al.

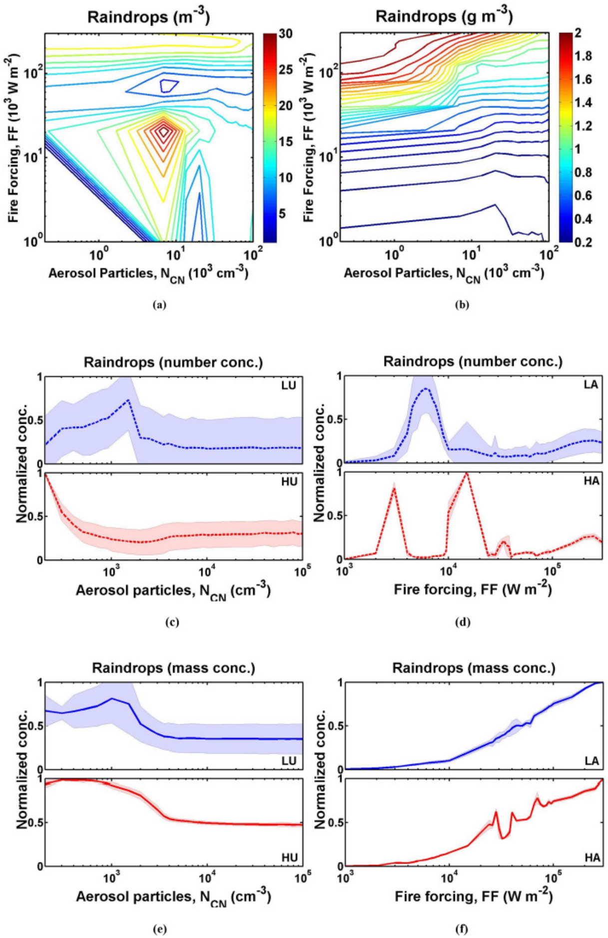


**Fig. 4.** Same as Fig. 2 but for raindrops.





ACPD
14, 7777–7822, 2014

Aerosol and dynamic effects on the formation of pyro-clouds

D. Chang et al.

Title Page
Abstract Introduction
Conclusions References
Tables Figures
◂ ▸
Back Close
Full Screen / Esc
Printer-friendly Version
Interactive Discussion

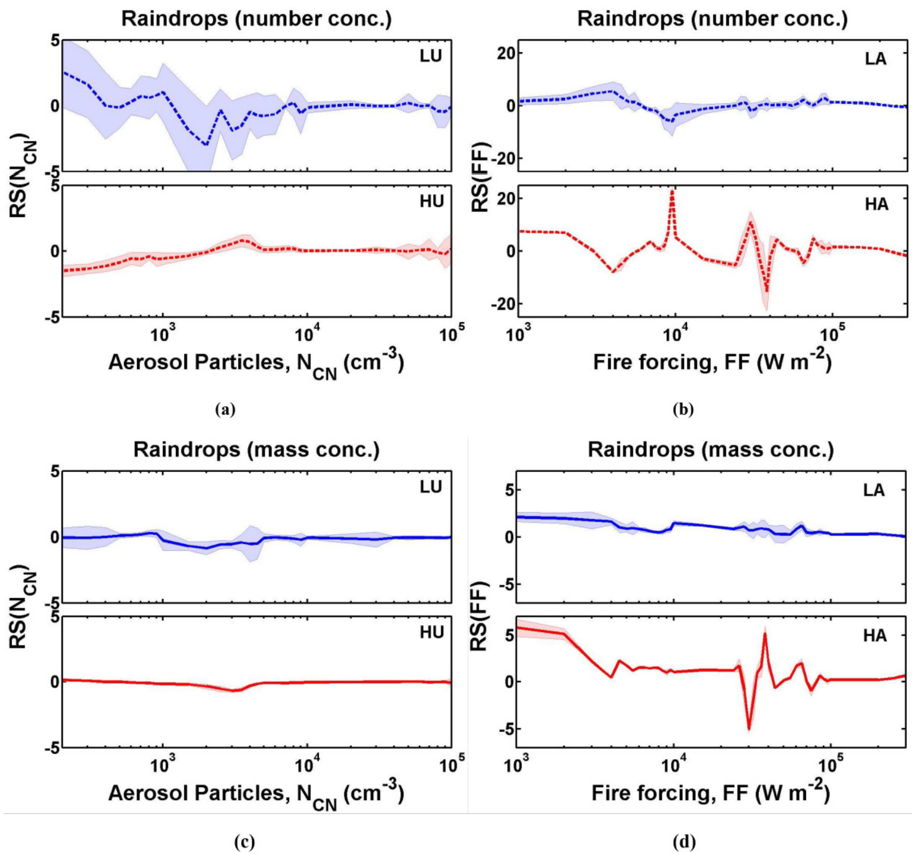


**Fig. 5.** Same as Fig. 3, but for raindrops.





ACPD
14, 7777–7822, 2014

Aerosol and dynamic effects on the formation of pyro-clouds

D. Chang et al.

Title Page
Abstract Introduction
Conclusions References
Tables Figures
◀ ▶
Back Close
Full Screen / Esc
Printer-friendly Version
Interactive Discussion

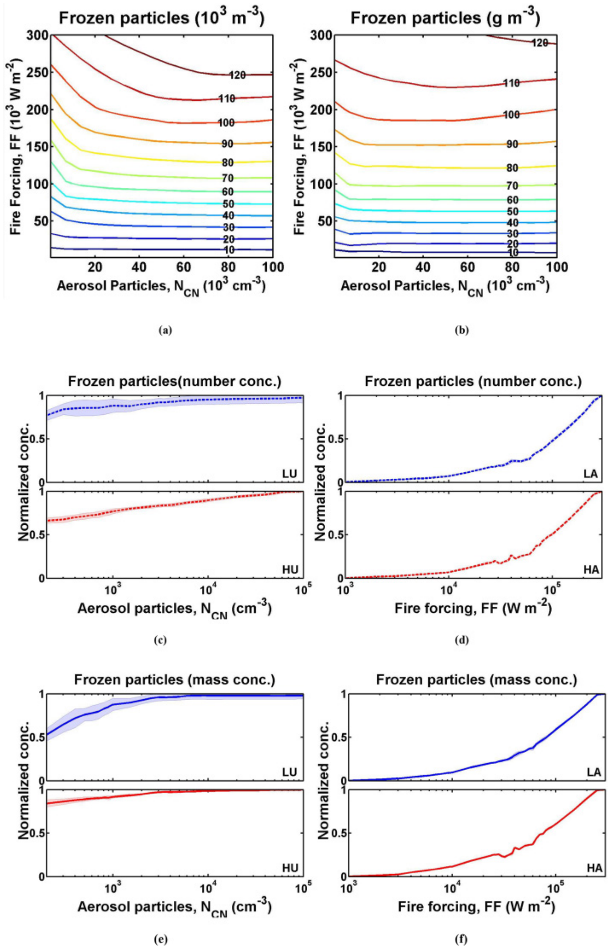


**Fig. 6.** Same as Fig. 2 but for total frozen particles.





ACPD
14, 7777–7822, 2014

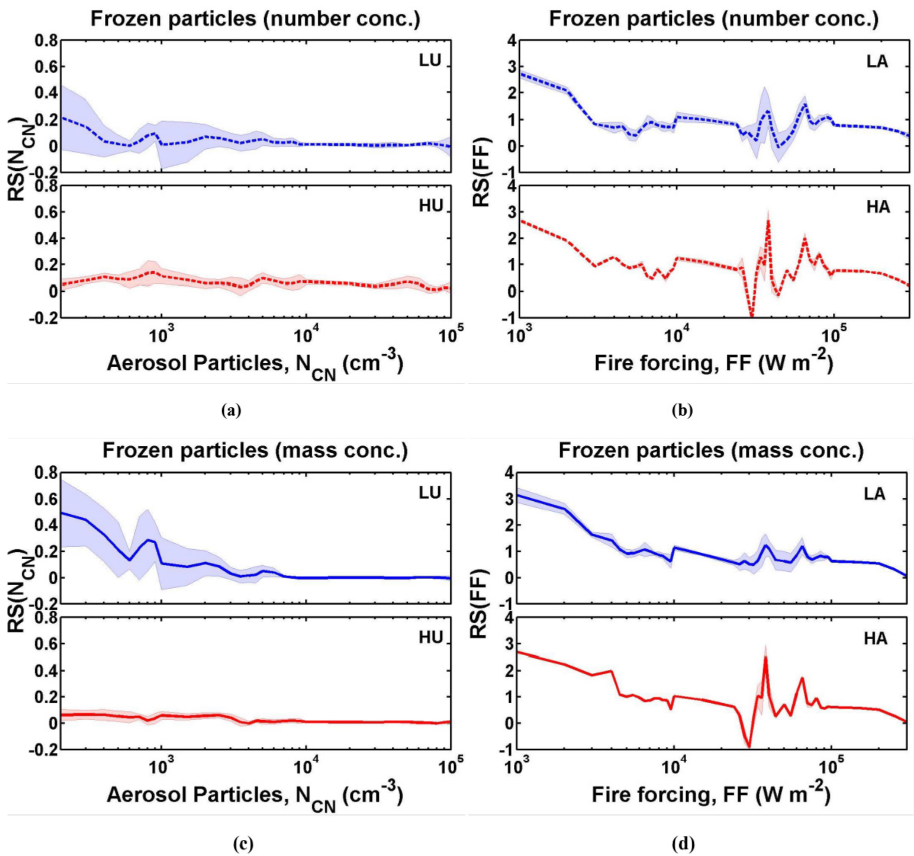


**Fig. 7.** Same as Fig. 3, but for frozen particles.





ACPD
14, 7777–7822, 2014

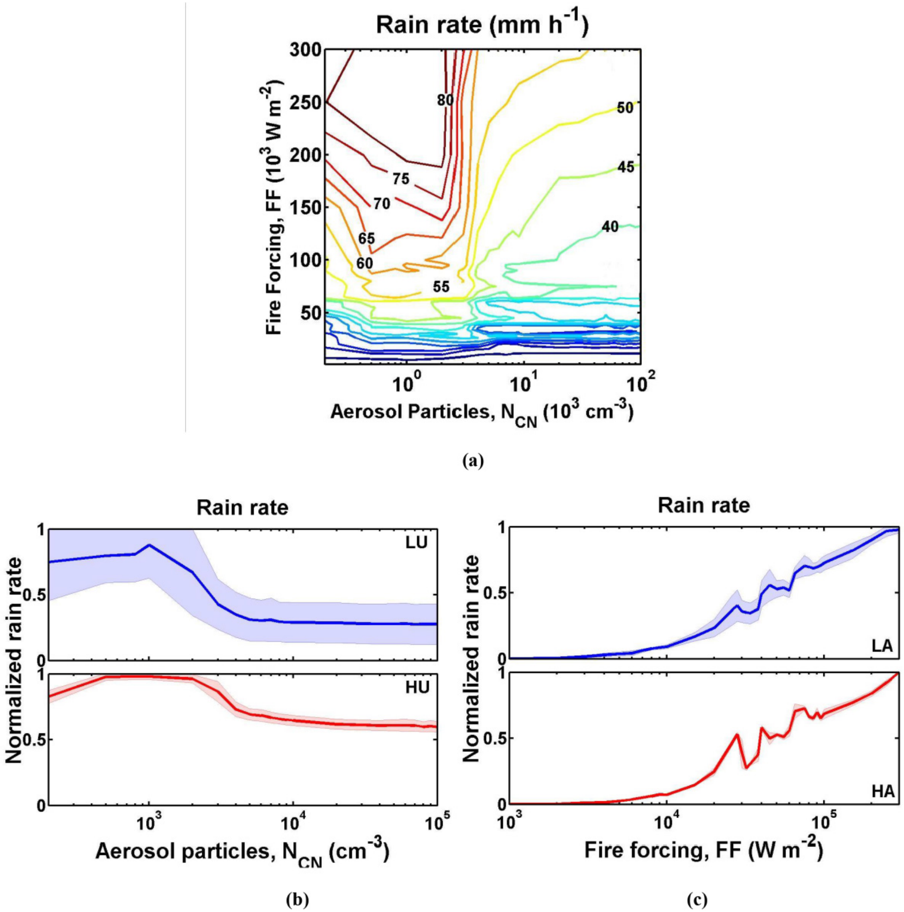


**Fig. 8.** Same as Fig. 2 but for surface rain rate.





ACPD
14, 7777–7822, 2014

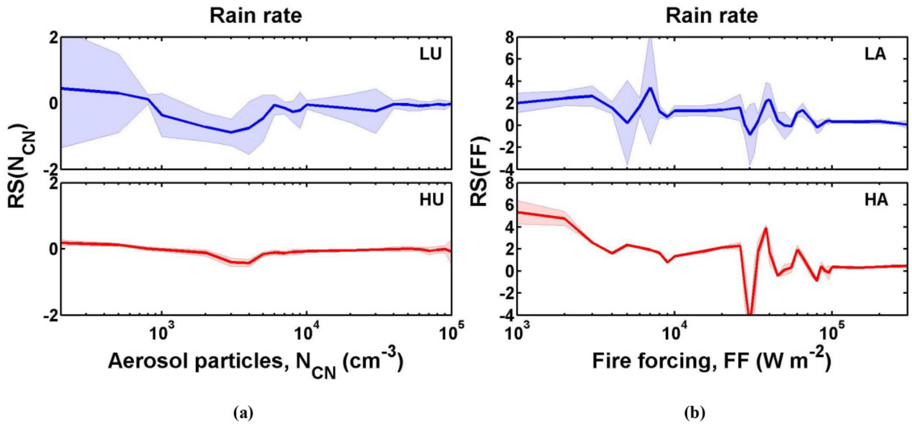


**Fig. 9.** Same as Fig. 3, but for surface rain rate.





ACPD
14, 7777–7822, 2014

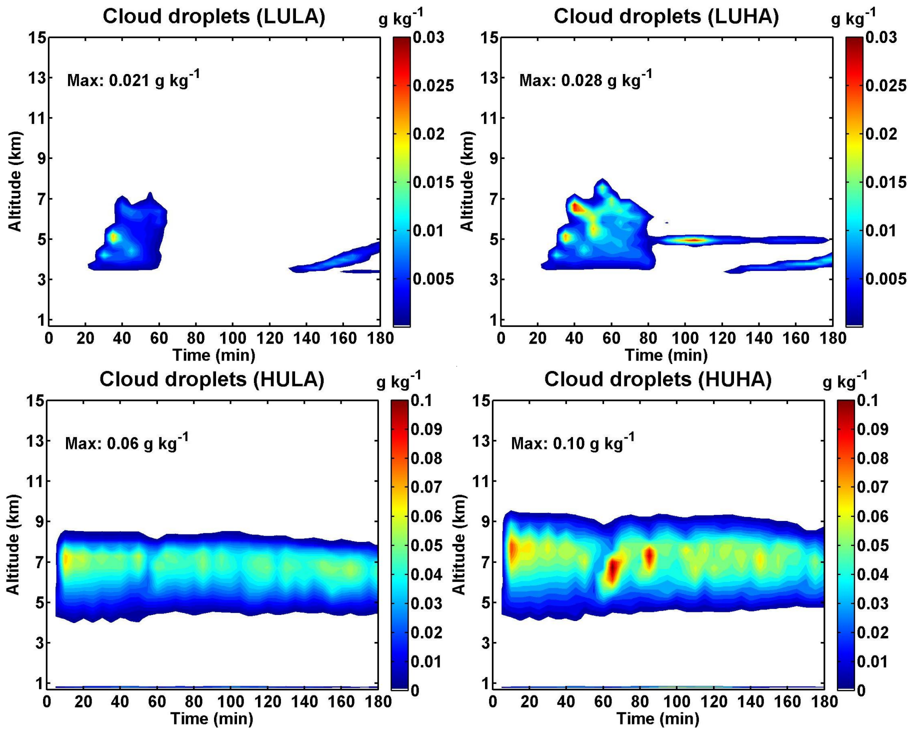


**Fig. 10.** Time evolution of horizontally-averaged cloud water content ($g\,kg^{-1}$) as a function of altitude for four extreme cases, which are referred to as (1) LULA: low updrafts ($2000\,W\,m^{-2}$) and low aerosols ($200\,cm^{-3}$); (2) LUHA: low updrafts ($2000\,W\,m^{-2}$) and high aerosols ($100\,000\,cm^{-3}$); (3) HULA: high updrafts ($300\,000\,W\,m^{-2}$) and low aerosols ($200\,cm^{-3}$); (4) HUHA: high updrafts ($300\,000\,W\,m^{-2}$) and high aerosols ($100\,000\,cm^{-3}$). Maximum values for each episode are also shown.





ACPD
14, 7777–7822, 2014

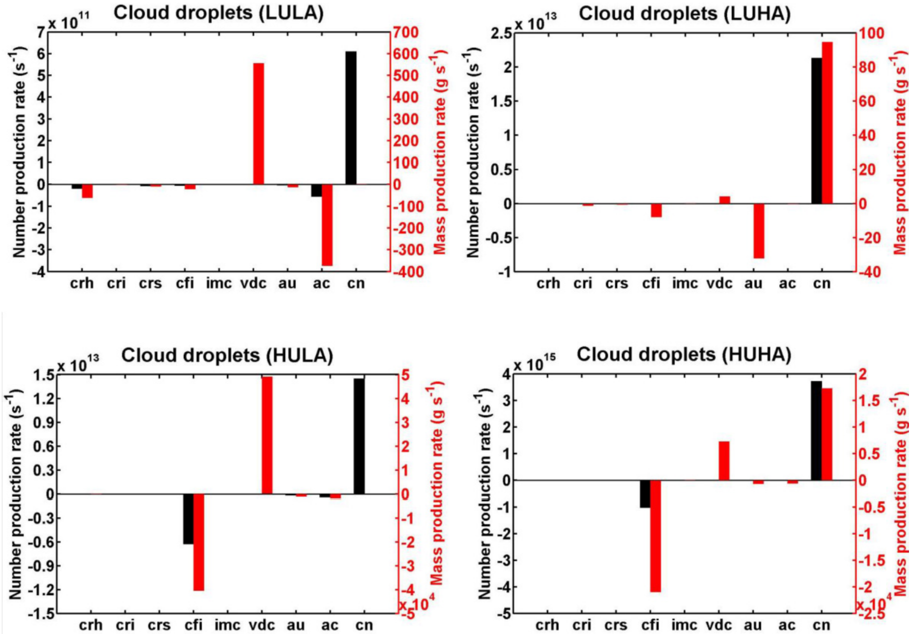


**Fig. 11.** Comparisons of the time-averaged rates of change in cloud droplet concentration resulting from the main processes, which were obtained from the domain-integrated values. Histograms indicate contributions of processes to number concentration (black) and mass concentration (red). Sources are plotted as positive values, and sinks are negative. The acronyms indicate crh/$i$/$s$: riming of cloud droplets to form hail/ice crystals/snow; imc: melting of ice crystals to form cloud water; vdc: depositional growth of cloud droplets; au: autoconversion; ac: accretion; cn: cloud nucleation.





ACPD
14, 7777–7822, 2014

Aerosol and dynamic effects on the formation of pyro-clouds

D. Chang et al.

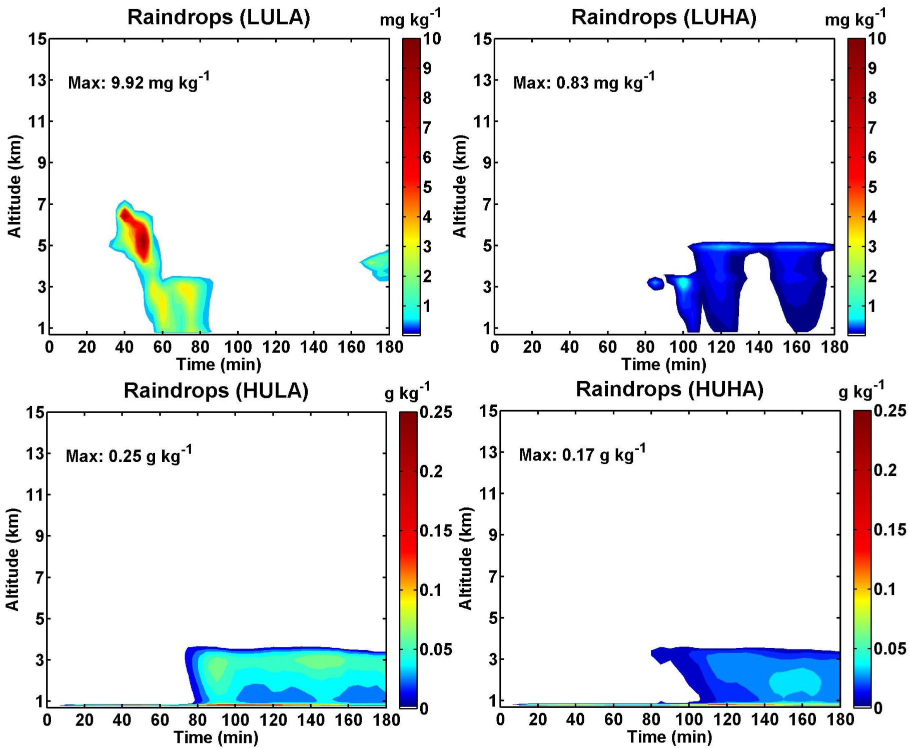


**Fig. 12.** Same as Fig. 10 but for raindrops.





ACPD
14, 7777–7822, 2014

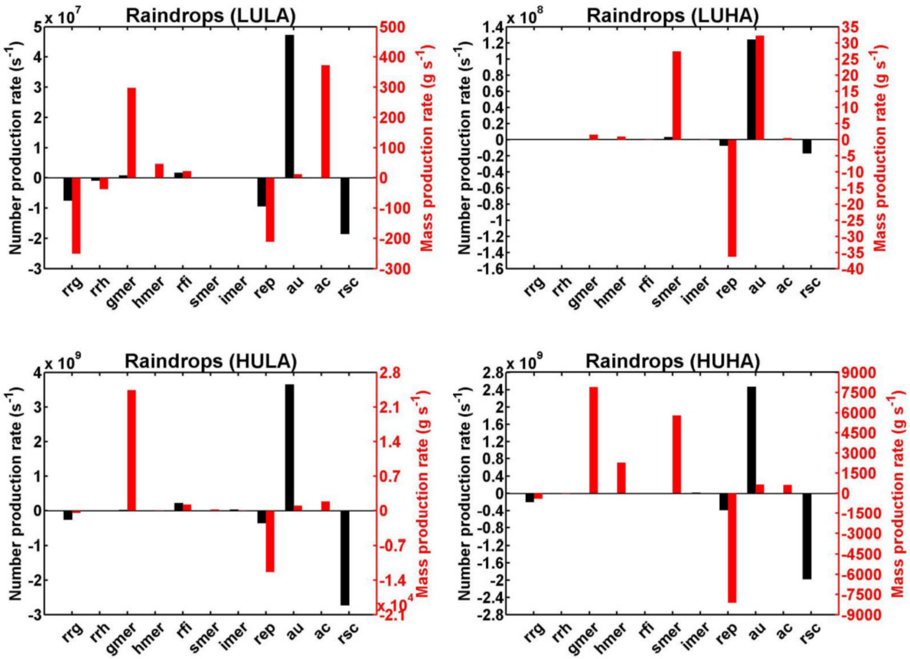


**Fig. 13.** Same as Fig. 11 but for raindrops. The acronyms indicate rrg/$h$: riming of rain to form graupel/hail; $g/h/s/$imer: graupel/hail/snow/ice multiplication to form ice crystals; rfi: freezing of raindrops to form ice crystals; rep: evaporation of rain; au: autoconversion; ac: accretion; rsc: self-collection of raindrops.





ACPD
14, 7777–7822, 2014

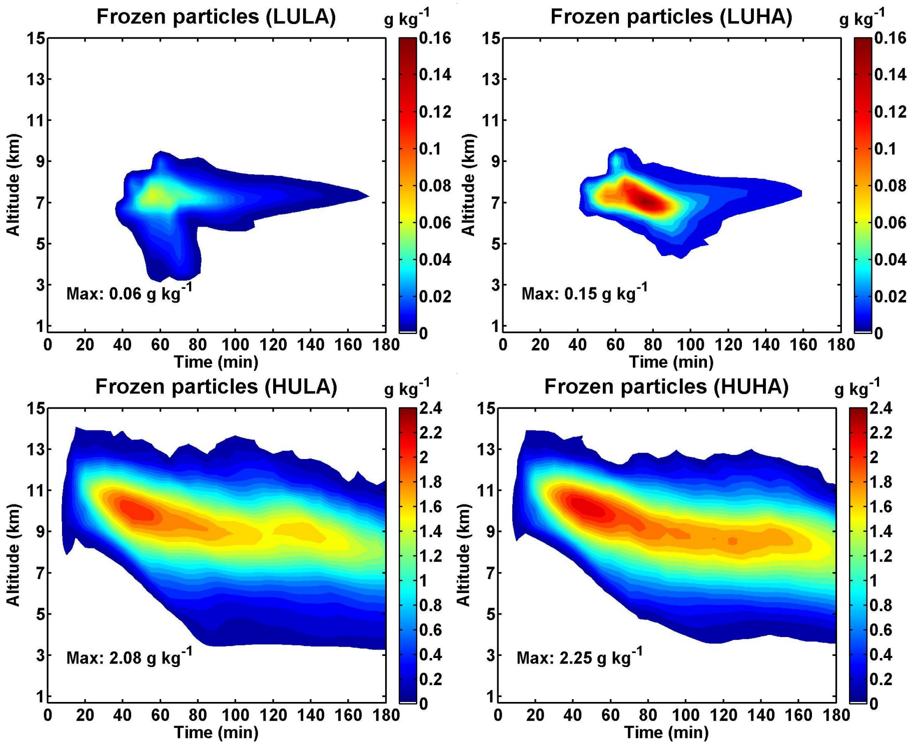


**Fig. 14.** Same as Fig. 10 but for the frozen particles.





ACPD
14, 7777–7822, 2014

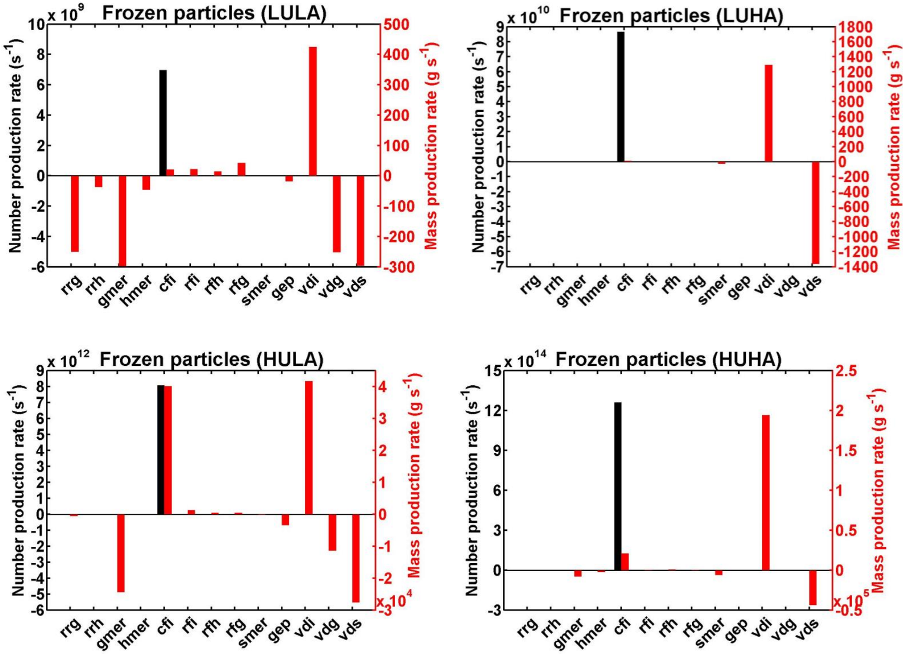


**Fig. 15.** Same as Fig. 11 but for the frozen particles. The acronyms indicate rrg/$h$: riming of rain to form graupel/hail; $g$/$h$/smer: graupel/hail/snow multiplication to form ice crystals; $c$/rfi: freezing of cloud water/raindrops to form ice crystals; rfh/$g$: freezing of raindrops to form hail/graupel; gep: evaporation of graupel; vdi/$g$/$s$: depositional growth of ice crystals/graupel/snow.





ACPD
14, 7777–7822, 2014